

## Non-Destructive Optical Monitoring for Calcification of Tissue-Engineered Bone *In Vitro*\*

Shigeo. M. TANAKA \*\*, Masafumi KAKIO \*\*\* and Ken-ich YAMAKOSHI \*\*\*

\*\*Institute of Nature and Environmental Technology, Kanazawa University,  
Kakuma-machi, Kanazawa, Ishikawa, Japan  
E-mail: shigeo@t.kanazawa-u.ac.jp

\*\*\*Graduate School of Natural and Science Technology, Kanazawa University,  
Kakuma-machi, Kanazawa, Ishikawa, Japan

### Abstract

In this study, a non destructive monitoring system for osteoblastic calcification in tissue-engineered bone *in vitro* was proposed and developed utilizing near-infrared light. The system consists of LEDs and a photo detector (PD) underneath a culture dish. The LED irradiates near-infrared light ( $I_0$ ) at 850 nm increasing its intensity to a tissue-engineered bone placed in the culture dish. The diffuse reflectance light ( $I$ ) from the engineered bone is detected by the PD and the degree of calcification is evaluated by the slope of  $I_0$ - $I$  curve. A steeper slope represents higher degree of calcification. This system was calibrated with type I collagen sponge scaffolds deposited artificially with hydroxyapatite and the degree of calcification was expressed in bulk density ( $\text{mg}/\text{cm}^3$ ). Using this system, osteoblastic calcification in tissue-engineered bones composed of the collagen sponge scaffold and rat-primary cultured osteoblasts or MC3T3-E1 cells was monitored for 42 days. The system succeeded not only in monitoring an increase in the bulk density of the engineered bones with the culture period, but also in distinguishing the difference of calcification ability between the cells, i.e., the higher ability of rat-primary cells and the lower ability of MC3T3-E1 cells, which could not be confirmed by the observation under visible light. The results suggested the efficacy of our system using near infrared light in long-term monitoring of oeteogenesis *in vitro*, by which this optical monitoring system could contribute to bone tissue engineering and to basic bone biology as well.

**Key words:** Tissue-Engineered Bone, Calcification, Optical Monitoring, Near Infrared Light, Non-Destructive, Osteoblasts, Collagen Sponge, In Vitro

### 1. Introduction

In bone tissue engineering, their own stem cells taken from patients are cultured and differentiated to osteoblasts, of which an artificially-regenerated bone is made with a scaffold *in vitro* prior to implantation. This technology has a potential not only to provide biocompatibility superior to previous biomaterials, but also to overcome the ethical problems in cadaveric donor transplantation and living donor transplantation. Many types of intervention such as physical or biochemical stimulations <sup>(1-10)</sup> have been studied and showed a potential to promote *in vitro* calcification of tissue-engineered bone. Optimization of stimulation condition is important to achieve successful promotion of the calcification, however, it is a time-consuming work with a repetition of examinations in every possible

\*Received 2 Apr., 2008 (No. 08-0274)  
[DOI: 10.1299/jbse.3.332]

condition. Moreover, since only destructive measurement methods are available currently for three-dimensional (3D) osteoblastic calcification<sup>(1,2,11-17)</sup>, an enormous number of samples have to be prepared. Non destructive ways should give us a more time- and work-saving investigation for this purpose. In two-dimensional (2D) culture, on the other hand, a non-destructive method using a visible light microscope and a digital image analyzer have been established<sup>(16,18)</sup>. However, visible lights can not penetrate easily into a calcified 3D matrix with high optical scattering, suggesting that this method is not applicable to tissue-engineered bones.

The objective of this study is to develop a non-invasive optical monitoring system for osteoblastic calcification in tissue-engineered bones utilizing a near-infrared light, which has higher penetrability to bio-tissues including bone than visible lights and been used in various non-invasive measurements *in vivo*<sup>(19)</sup>. As near-infrared light is scattered more by highly calcified bone matrix<sup>(20)</sup>, our system can evaluate the degree of calcification of a tissue-engineered bone by detecting diffuse reflectance light from the bone. This system was designed and finished in small and low cost by using commercially-available optical devices, i.e., light emitting diodes (LED) and a photo detector (PD). In this study, to verify the efficacy of the developed system, a long-term monitoring was performed for two types of tissue-engineered bone with different osteoblasts.

## 2. Materials and Methods

### 2.1 Optical monitoring system

The system consists of four LEDs (Epitex, L850-40M32) and a Germanium-type PD (Judson, J16-5SP-R03M-SC) surrounded by the LEDs underneath a culture dish (Fig. 1). The gap between the tip of these optical devices and the bottom surface of tissue-engineered bone placed on the culture dish is 2.6 mm including the 1.6-mm thickness of culture plate. The radiation angle of the LED is  $\pm 10^\circ$  with light intensities over 70% of the maximum at the center. With the small gap, the narrow radiation angle, and four LEDs, the bone can be irradiated as large area as possible without light leakage outside of the bone area. In this system, the LEDs emit near-infrared light to a tissue-engineered bone increasing linearly its intensity ( $I_0$ ) at 850 nm, and the diffuse reflectance light ( $I$ ) from the bone is detected by the PD. The degree of calcification is evaluated using the slope of  $I_0$ - $I$  curve (Fig. 2a). In the case of higher degree of calcification, the slope becomes steeper (Fig. 2b). The slope of  $I_0$ - $I$  curve also depends on the configuration of the optical unit and the properties of LEDs and PD. By using the slope, this evaluation has robustness to the variation of background light level. Light emission intensity of LED was controlled by a computer (PC, Dell Inspiron 2200) through an AD/DA interface board (National Instruments, DAQ Card-6036E, 16-bit resolution) with applied currents from 0 to 31 mA. Detected signal by the PD was transferred to the PC via an amplifier (Hamamatsu Photonics, c9329) and the interface board, and then the voltage value detected was used as " $I$ ". With  $I_0$  calibrated in advance, an  $I_0$ - $I$  curve was made with 9000 data points on the PC. The PC was operated by a program written by Visual Basic (Microsoft). A slope was obtained from a regression line for available all data points except those saturated in a range up to 5 V.

To calibrate this system, type I collagen sponge scaffolds (Zimmer Dental Inc., CollaCote, L20mm  $\times$  W16mm  $\times$  t2mm, pore size: about 100  $\mu$ m) deposited with hydroxyapatite (HA) were prepared<sup>(4)</sup> adjusting its bulk density from 0 to about 130 mg/cm<sup>3</sup>, which is determined by the dry weight divided by the bulk volume of the scaffold. The slope of  $I_0$ - $I$  curve correlated positively with the bulk density of HA-deposited sponge with a high correlation coefficient ( $r^2$ ) of 0.927 (Fig. 3a).

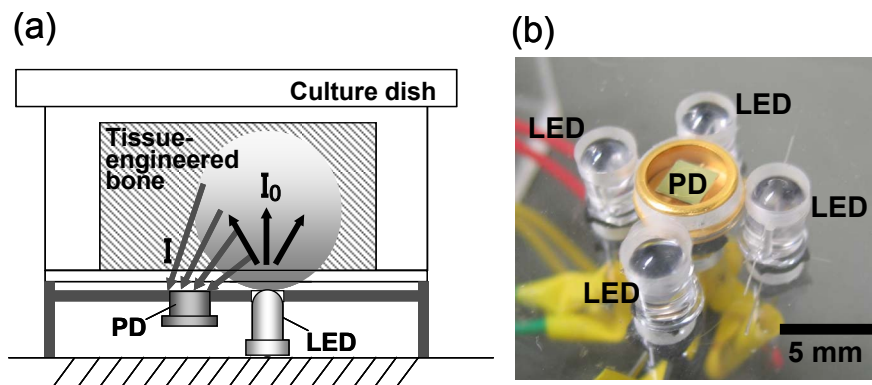


Fig. 1 Optical monitoring system for the calcification of tissue-engineered bone. (a) Tissue-engineered bone on a culture dish is irradiated with near-infrared light (850 nm) from LEDs at an intensity of  $I_0$ . Diffuse reflective light from the bone is detected by a PD at an intensity of  $I$ . (b) Optical sensing unit composed of four LEDs and one PD.

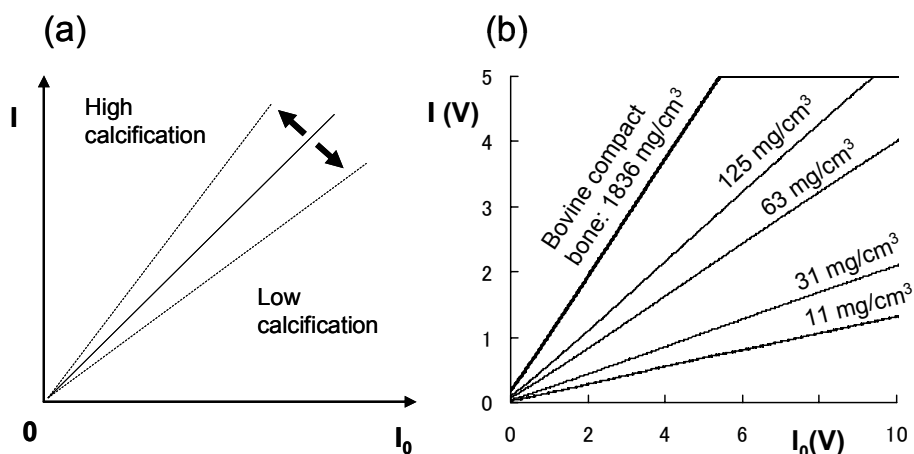


Fig. 2 (a)  $I_0$ - $I$  curve with a slope representing the degree of calcification. (b) Typical  $I$ - $I_0$  curves for HA-deposited collagen sponges with varied bulk density and a compact bone sample with a 2-mm thickness, taken from a bovine femur.

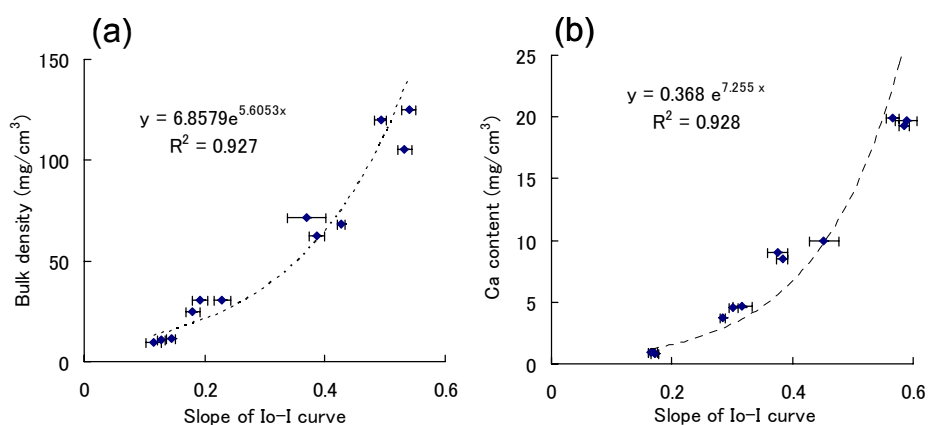


Fig. 3 Relationship between the slopes of  $I_0$ - $I$  curve and the bulk densities (a) or the calcium contents (b) of HA-deposited collagen sponge scaffold. Data represent the mean  $\pm$  SD for six (a)- or four (b)-time measurements.

In this study, using the regression curve for this relation ( $y = 6.8579e^{5.6053x}$ ) as a calibration curve, the degree of calcification of tissue-engineered bone was estimated and expressed as bulk density ( $\text{mg}/\text{cm}^3$ ). That is to say, in this study, "the degree of calcification" of tissue-engineered bone was defined and treated as an equivalent value to the bulk density of HA-deposited scaffold.

## 2.2 Optical monitoring for tissue-engineered bone

Osteoblasts were derived from mesenchymal stem cells in bone marrow, which were taken from the femurs of 12-week old female rats, referring to the procedure reported by Maniatopoulos et al <sup>(17)</sup>. The stem cells were pre-cultured in osteogenic differentiation medium <sup>(17)</sup>, which is  $\alpha$ -modified minimum essential medium ( $\alpha$ -MEM, Sigma) containing 10% fetal bovine serum (FBS), 1% antibiotics cocktail (100 U/ml penicillin and 100  $\mu\text{g}/\text{ml}$  streptomycin, Invitrogen), 50  $\mu\text{g}/\text{ml}$  L-ascorbic acid (Sigma),  $10^{-8}\text{M}$  dexamethasone (Sigma), and 10 mM  $\beta$ -glycerophosphate (Sigma) for 7-10 days. After the pre-culture,  $0.5 \times 10^6$  osteoblasts were seeded into each collagen sponge scaffold mentioned above. To ensure stable monitoring in long-term culture, the two opposite side walls of scaffold were adhered with silicon rubber glue (Dow Corning) to square plastic sticks fixed on the bottom surface of a polystyrene  $\phi 35$  mm-culture dish (Falcon, 3502). The optical monitoring for the tissue-engineered bones were performed at day 1, 3, 7, 14, 21, 28, 35, and 42 after the seeding ( $n = 4$ ). On the same observation days, close-up photography using a digital camera (Canon, A95) was also carried out for the engineered bones. As a comparative sample, tissue-engineered bones populated by the established osteoblastic cell line (MC3T3-E1) cells <sup>(21)</sup> were tested as well with  $\alpha$ -MEM containing 10% FBS and 1% antibiotics only. This type of osteoblast is known to show little calcification under the normal culture condition <sup>(14)</sup>. A paired t-test was conducted to examine statistical significance between these two types of tissue engineered bone. Statistical significance was evaluated if the p-value was 0.05 or lower.

## 2.3 Histological observation of cells in tissue-engineered bone

To observe the distribution of the osteoblasts seeded in the scaffold, Hematoxylin-Eosin (HE) staining was performed for the tissue-engineered bone with MC3T3-E1 cells. The engineered bone was taken out of culture dish 24 hours after the seeding and fixed with 100-mM cacodylate buffer containing 2% paraphormaldehyde and 2% glutaraldehyde for 12 hours. The sample was then dehydrated in a series of graded ethyl alcohols, embedded in paraffin, sectioned at 5  $\mu\text{m}$  in thickness and stained by HE. Scanning electron microscopy (SEM) was performed to observe the morphology of osteoblasts in the scaffold. After the primary fixation, the sample was rinsed in 0.1M phosphate buffer several times and then dehydrated through a series of graded ethyl alcohols. The sample in 100% alcohol was frozen using liquid nitrogen and fractured. The fractured sample was then re-hydrated and post fixed with 1% osmium tetroxid in 0.1M phosphate buffer for 1-2 hours, and dehydrated in a series of graded ethyl alcohols. The sample was dried using a critical point dryer (Tousimis Research Co., Samdri-780), and coated with gold-palladium by sputter deposition (Anatech Ltd., Hummer V). Scanning electron microscopy (KLA-Tencor, Amray 1000A) was performed for the fracture plane of the sample at 20 kV.

## 2.4 Colorimetric quantitative evaluation of calcification

To confirm the reliability of our system, separately from the optical monitoring, a colorimetric quantitative method was performed for the tissue-engineered bone samples calcified by the primary-cultured osteoblasts. This established method detects calcium content solved in liquid. On each observation day (day 1, 3, 7, 14, 21, 28, and 35 after seeding), an engineered bone was taken out of the culture dish, dissolved in 1ml of 1 N



HCl, and then frozen at -20 °C. The frozen sample was homogenized using a plastic stick to get further solubility. The sample solution was centrifuged and separated into supernatant and scaffold debris. Calcium content in the supernatant was quantified using a kit (Calcium E-Test Wako Kit, Wako Chemicals) based on the ortho-cresolphthalein complexone (OCPC) method and a photospectrometer (Hitachi, U-1900), according to the manufacturer's instructions. Standards were also prepared in 1 N HCl and calcium content was expressed in mg per the apparent volume of scaffold. Fig. 3b shows the relationship between the slopes of  $I_0$ -I curve and calcium contents measured for HA-deposited collagen sponges described above, representing a similar tendency to the relationship between the slope and the bulk density (Fig. 3a).

### 3. Results

Fig. 4a shows a typical HE stained section image taken from the center section at about 1 mm in depth from the surface of the scaffold. The osteoblasts were apparently extended their processes and connected to each other making a cellular network. The SEM images in the similar site represented that the cells were anchored and settled down on the surface of matrix (Fig. 4b).

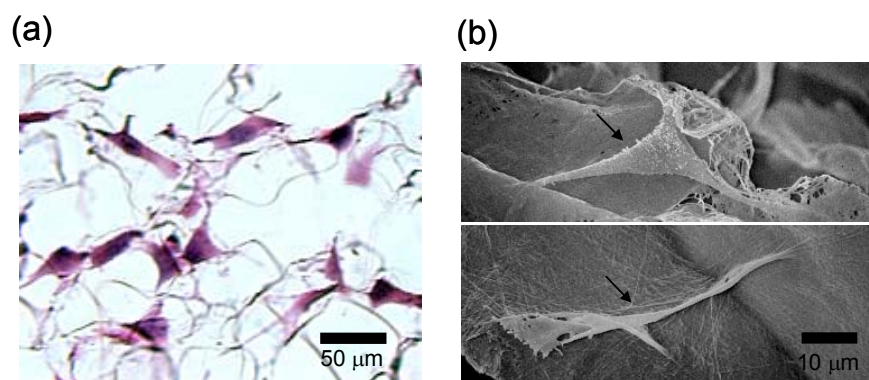


Fig. 4 Histology of osteoblasts (MC3T3-E1 cells) in a collagen sponge scaffold. (a) The image of a HE stained section, representing the distribution of osteoblasts in the scaffold. (b) SEM image of osteoblasts on the surface of the scaffold (freeze-fracturing method). The arrow points osteoblasts.

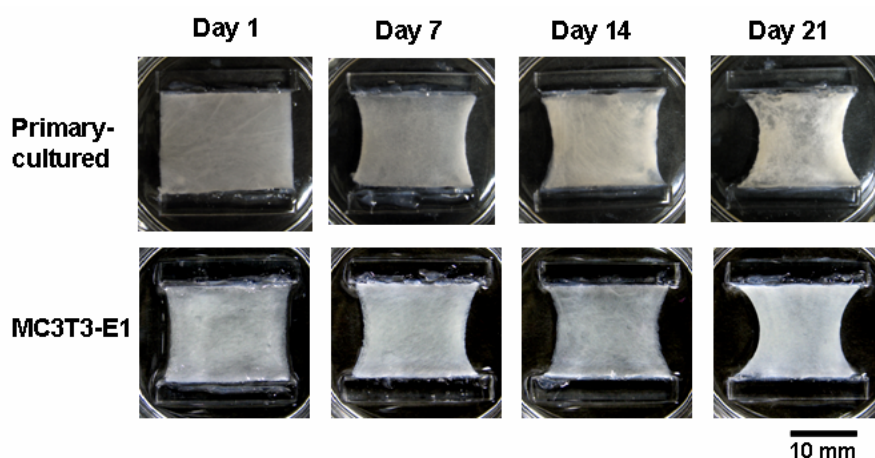


Fig. 5 Close-up photographic images of the tissue-engineered bones, showing changes in the appearance of the tissue-engineered bones with the rat primary-cultured osteoblasts cells or MC3T3-E1 cells with days in culture.

Fig. 5 shows close-up photographic images, representing changes in appearance of the tissue-engineered bones by day 21. From these images taken under visible light, changes in calcification of the engineered bones with culture period could not be confirmed clearly as well as differences of calcification between both cells. Larger shrinkage of the engineered bone, which is caused by cellular contraction force, was observed in longer culture periods either in the primary-cultured osteoblasts or in MC3T3-E1 cells. However, no difference of shrinkage was detected between these two cells. After day 21, the appearance of both engineered bones became stable and did not show any remarkable change.

Fig. 6 shows changes in the bulk density of the tissue-engineered bones with culture period, monitored by the optical monitoring system. In the tissue-engineered bone with the primary-cultured osteoblasts, the density started to increase linearly after day 7 and reached to about 55 mg/cm<sup>3</sup> at day 42. On the other hand, the engineered bone with MC3T3-E1 cells did not represent an increase in bulk density. Calcium content of the tissue-engineered bone measured by the colorimetric quantitative method correlated with the bulk density of the bone predicted by the optical monitoring system with a high correlation coefficient ( $r^2 = 0.9018$ ) (Fig. 7), suggesting the reliability of the optical system.

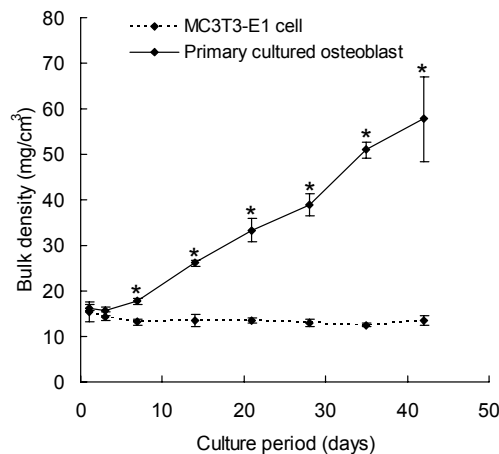


Fig. 6 Changes in the bulk density of the tissue-engineered bones with culture period. Solid line: primary-cultured osteoblasts, Dash line: MC3T3-E1 cells. Data represent the mean  $\pm$  SD (n = 4). \*p < 0.0001 versus MC3T3-E1.

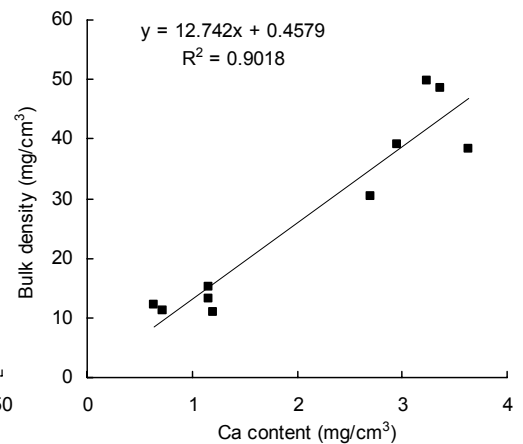


Fig. 7 Relationship between the bulk density of the tissue-engineered bone predicted by the optical system and calcium content measured by the colorimetric quantitative method

#### 4. Discussion

Our optical system succeeded in non-destructive monitoring for the calcification of the tissue-engineered bones for 42 days in culture. By utilizing near-infrared light, the system could distinguish between uncalcified and calcified scaffold, on the other hand, the close-up photographic observation under visible light failed.

Previously, only destructive ways such as histochemistry (Alzarin red <sup>(11-13)</sup>, and von Kossa <sup>(14,15)</sup> staining method), colorimetric quantitative method <sup>(1,2)</sup>, flame atomic absorption spectrometry <sup>(16)</sup>, Fourier transform infrared (FTIR) <sup>(16)</sup>, and X-ray diffraction <sup>(17)</sup> were available and employed to evaluate the calcification induced by osteoblasts *in vitro*. In these destructive methods, to follow precise changes in calcification for long-term in culture, many samples and time points for observation have to be prepared, forcing us inefficient works. On the other hand, a non-destructive method has been used only for 2D culture studies, in which mineralized nodules on the surface of culture dish are counted by a mean

of microscopic digital image analyzer<sup>(16,18)</sup>. However, this method can not be applicable to the detection of calcification in 3D culture, because visible lights can not penetrate to a 3D matrix due to reflection and scattering on the surface of scaffold. For this reason, in this study, the close-up photography using a digital camera could not recognize the difference of the degree of calcification as shown in Fig. 5.

Near infrared light used in our system can penetrate the scaffold easily, so that diffuse reflectance light delivers the information of calcification inside of the scaffold to the PD detector. With its deep penetration and safety aspects for living tissues, near-infrared light is often utilized and studied in application for non-invasive biomedical sensing technology, e.g., pulse oximetry<sup>(22,23)</sup>, glucometry<sup>(24-26)</sup>, blood pressure measurement<sup>(27,28)</sup>, or bone densitometry<sup>(29-31)</sup>. In our system, the slope of  $I_0$ -I curve was used as a parameter to evaluate calcification. This parameter is not only better at robustness for background variation, but also provides a wider dynamic range, up to the highest calcification observed in a compact bone (Fig. 2b), compared with conventional optical measurements using only one incident light intensity. However, this parameter depends essentially on the thickness of scaffold, therefore, different calibration curves should be prepared for the different thicknesses of scaffold. Our results demonstrated the shrinkage of tissue-engineered bones in culture (Fig. 5), which would be caused by the cellular contraction force of osteoblasts proliferating in a scaffold, showing decrease in the thickness of scaffold. Cellular contraction force has been reported in fibroblasts<sup>(32-34)</sup>, known to induce the shrinkage of scaffold<sup>(30)</sup>, and plays an important role in tissue wound healing<sup>(35)</sup>. Nevertheless, the relationship between the slopes of  $I_0$ -I curve and the bulk densities of scaffold was not affected significantly by the change in thickness of scaffold, ranging from 0.5 to 2.0 mm, in HA-deposited samples (Fig. 8). The average of errors from bulk densities predicted by the calibration curve (Fig. 3a) was 7.47 mg/cm<sup>3</sup>. For more accurate monitoring, it would be necessary to employ stiffer scaffolds and/or other techniques able to cancel the thickness effect. The optical coherence tomography (OCT)<sup>(36,37)</sup> with a high depth resolution of  $\mu$ m order could be one of the candidate techniques. However, a simpler and lower cost system, e.g., depth-resolved spectroscopy<sup>(38)</sup>, would be more desirable only for the purpose of detection of the degree of calcification, rather than OCT.

In this study, the degree of calcification of tissue-engineered bone was evaluated as an equivalent value to the bulk density of HA-deposited scaffold. It should be noted that a predicted bulk density could be overestimated due to the optical scattering of proteins, e.g., type I collagen, expressed by osteoblasts in a tissue-engineered bone. However, major reflected light should come from calcified matrix and the scattering effect of proteins seems to be minor, because the optical scattering coefficient ( $\mu_s$ ) of skin tissue made of type I collagen is 2- to 3-fold smaller than that of bone matrix<sup>(20, 39)</sup>. Also, the shrinkage of tissue-engineered bone by cellular contraction force should increase the intensity of reflection light, resulting in an increase in the slope of  $I_0$ -I curve, by which the degree of calcification could be overestimated. The degree of calcification defined in this study could be increased not only by an increase in HA deposition to scaffold matrix, but also in other cellular activities, such as protein expression, contraction force generation, and so on.

In the tissue-engineered bone with the rat primary-cultured osteoblasts, the bulk density reached about 55 mg/cm<sup>3</sup> at day 42 in culture. This density, however, is one-third and a half of the density of trabecular bone in young normal and osteoporotic woman, respectively<sup>(40)</sup>. Some interventions such as mechanical<sup>(1-4)</sup>, electrical<sup>(5,6)</sup>, electromagnetic<sup>(7,8)</sup>, or biochemical<sup>(9,10)</sup> stimulation would be expected to give more calcification to the engineered bone.



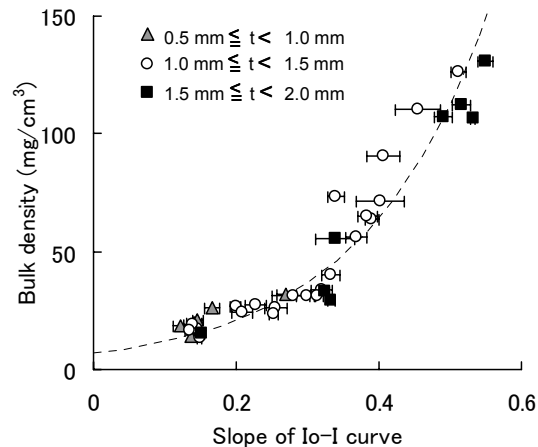


Fig. 8 Relationship between the slopes of  $I_0$ -I curve and the bulk densities of HA-deposited collagen sponge scaffold with a thickness varied in a range from 0.5 to 2.0 mm. The dashed line indicates the calibration curve ( $y = 6.8579e^{5.6053x}$ , Fig. 3a) used for the calcification monitoring. Data represent the mean  $\pm$  SD for four-time measurements.

## 5. Conclusion

An optical monitoring system for the calcification of tissue-engineered bone *in vitro* was developed and applied to those made of a collagen sponge scaffold and rat primary-cultured osteoblasts or MC3T3-E1 cells. The results suggested the efficacy of this system in long-term monitoring. Our system could contribute not only to the progress of bone tissue engineering, but also to basic researches on bone biology.

## Acknowledgments

This research was partially supported by the Ministry of Education, Science, Sports and Culture, Grant-in-Aid for Scientific Research (C), 18500343, 2006-7. We are grateful to Keith W. Condon and Caroline A. Miller in Department of Anatomy, School of Medicine, Indiana University for their helps in the histological studies.

## References

- (1) Bancroft, G.N., Sikavitsas, V.I., van den Dolder, J., Sheffield, T.L., Ambrose, C.G., Jansen, J.A., and Mikos, A.G., Fluid flow increases mineralized matrix deposition in 3D perfusion culture of marrow stromal osteoblasts in a dose-dependent manner, *Proceedings of the National Academy of Sciences of the United States of America*, Vol. 99, No. 20 (2002), pp. 12600-12605.
- (2) van den Dolder, J., Bancroft, G.N., Sikavitsas, V.I., Spauwen, P.H.M., Jansen, J.A., and Mikos, A.G., Flow perfusion culture of marrow stromal osteoblasts in titanium fiber mesh, *Journal of Biomedical Materials Research. Part A*, Vol. 64, No. 2 (2003), pp. 235-241.
- (3) Tanaka, S.M., Li, J., Duncan, R.L., Yokota, H., Burr, D.B., and Turner, C.H., Effects of broad frequency vibration on cultured osteoblasts, *Journal of Biomechanics*, Vol. 36, No. 1 (2003), pp. 73-80.
- (4) Tanaka, S.M., Sun, H.B., Roeder, R.K., Burr, D.B., Turner, C.H., and Yokota, H., Osteoblast responses one hour after load-induced fluid flow in a three-dimensional porous matrix, *Calcified Tissue International*, Vol. 76 (2005), pp. 261-271.
- (5) Zhuang, H., Wang, W., Seldes, R.M., Tahernia, A.D., Fan, H., and Brighton, C.T., Electrical



- stimulation induces the level of TGF-beta1 mRNA in osteoblastic cells by a mechanism involving calcium/calmodulin pathway, *Biochemical and Biophysical Research Communications*, Vol. 237, No. 2 (1997), pp. 225-229.
- (6) Wiesmann, H., Hartig, M., Stratmann, U., Meyer, U., and Joos, U., Electrical stimulation influences mineral formation of osteoblast-like cells in vitro, *Biochimica et Biophysica Acta.*, Vol. 1538, No. 1 (2001), pp. 28-37.
- (7) Heermeier, K., Spanner, M., Träger, J., Gradinger, R., Strauss, P.G., Kraus, W., and Schmidt, J., Effects of extremely low frequency electromagnetic field (EMF) on collagen type I mRNA expression and extracellular matrix synthesis of human osteoblastic cells, *Bioelectromagnetics*, Vol. 19, No. 4 (1998), pp. 222-231.
- (8) Lohmann, C.H., Schwartz, Z., Liu, Y., Li, Z., Simon, B.J., Sylvia, V.L., Dean, D.D., Bonewald, L.F., Donahue, H.J., and Boyan, B.D., Pulsed electromagnetic fields affect phenotype and connexin 43 protein expression in MLO-Y4 osteocyte-like cells and ROS 17/2.8 osteoblast-like cells, *Journal of Orthopaedic Research*, Vol. 21, No. 2 (2003), pp. 326-334.
- (9) Lu, H.H., Kofron, M.D., El-Amin, S.F., Attawia, M.A., and Laurencin, C.T., In vitro bone formation using muscle-derived cells: a new paradigm for bone tissue engineering using polymer-bone morphogenetic protein matrices, *Biochemical and Biophysical Research Communications*, Vol. 305, No. 4 (2003), pp. 882-889.
- (10) Lieb, E., Vogel, T., Milz, S., Dauner, M., and Schulz, M.B., Effects of transforming growth factor beta1 on bonelike tissue formation in three-dimensional cell culture. II: Osteoblastic differentiation, *Tissue Engineering*, Vol. 10, No. 9-10 (2004), pp. 1414-1425.
- (11) Doi, M., Nagano, A., and Nakamura, Y., Genome-wide screening by cDNA microarray of genes associated with matrix mineralization by human mesenchymal stem cells in vitro, *Biochemical and Biophysical Research Communications*, Vol. 290, No. 1 (2002), pp. 381-390.
- (12) Zhao, Y., Guan, H., Liu, S.F., Wu R.C., and Wang, Z.: Overexpression of QM induces cell differentiation and mineralization in MC3T3-E1, *Biological & Pharmaceutical Bulletin*, Vol. 28, No. 8 (2005), pp. 1371-1376.
- (13) Subramaniam, M., Gorny, G., Johnsen, S.A., Monroe, D.G., Evans, G.L., Fraser, D.G., Rickard, D.J., Rasmussen, K., van Deursen, J.M., Turner, R.T., Oursler, M.J., and Spelsberg, T.C., TIEG1 null mouse-derived osteoblasts are defective in mineralization and in support of osteoclast differentiation in vitro, *Molecular and Cellular Biology*. Vol. 25, No. 3 (2005), pp. 1191-9.
- (14) Bonewald, L.F., Harris, S.E., Rosser, J., Dallas, M.R., Dallas, S.L., Camacho, N.P., Boyan, B., and Boskey, A., von Kossa staining alone is not sufficient to confirm that mineralization in vitro represents bone formation, *Calcified Tissue International.*, Vol. 72, No. 5 (2003), pp. 537-547.
- (15) Ueno, A., Yamashita, K., Miyashi, K., Horiguchi, T., Ruspita, I., Abe, K., and Noma, T., Soluble matrix from osteoblastic cells induces mineralization by dental pulp cells, *The Journal of Medical Investigation*, Vol. 53 (2006), pp. 297-303.
- (16) Verberckmades, S.C., De Broe, M.E., and D'Haese, P.C., Dose-dependent effects of strontium on osteoblast function and mineralization, *Kidney International*, Vol. 64 (2003), pp. 534-543.
- (17) Maniopoulos, C., Sodek, J., and Melcher, A.H., Bone formation in vitro by stromal cells obtained from bone marrow of young adult rats, *Cell and Tissue Research*, Vol. 254 (1988), pp. 317-30.
- (18) Barbara, A., Delannoy, P., Denis, B.G., and Marie, P.J., Normal matrix mineralization induced by strontium ranelate in MC3T3-E1 osteogenic cells, *Metabolism*, Vol. 53, No. 4 (2004), pp. 532-537.
- (19) Rolfe, P., In vivo near-infrared spectroscopy, *Annual Review of Biomedical Engineering*, Vol. 2 (2000), pp. 715-754.
- (20) Ugryumova, N., Matcher, S.J., and Attenburrow, D.P., Measurement of bone mineral density

- via light scattering, *Physics in Medicine and Biology*, Vol. 49 (2004), pp. 469-483.
- (21) Kodama, H., Amagai, Y., Sudo, H., Kasai, S., and Yamanoto, S., Establishment of a clonal osteogenic cell line from newborn mouse calvaria, *Japanese Journal of Oral Biosciences*, Vol. 23 (1981), pp.899-901
- (22) Kiening, K.L., Unterberg, A.W., Bardt, T.F., Schneider, G.H., and Lanksch, W.R., Monitoring of cerebral oxygenation in patients with severe head injuries: brain tissue PO<sub>2</sub> versus jugular vein oxygen saturation, *Journal of Neurosurgery*, Vol. 85, No. 5 (1996), pp. 751-757.
- (23) Dawson, J.A., Davis, P.G., O'Donnell, C.P., Kamlin, C.O., and Morley, C.J., Pulse oximetry for monitoring infants in the delivery room: a review, *Archives of Disease in Childhood. Fetal and Neonatal Edition*, Vol. 92, No. 1 (2007), pp. F4-7.
- (24) Robinson, M.R., Eaton, R.P., Haaland, D.M., Koepp, G.W., Thomas, E.V., Stallard, B.R., and Robinson, P.L., Noninvasive glucose monitoring in diabetic patients: a preliminary evaluation, *Clinical Chemistry*. Vol. 38, No. 9 (1992), pp. 1618-1622.
- (25) Yamakoshi, K. and Yamakoshi, Y., Pulse glucometry: A new approach for noninvasive blood glucose measurement using instantaneous differential near-infrared spectrophotometry, *Journal of Biomedical Optics*, Vol. 11, No. 5 (2006), p.054028.
- (26) Maruo, K., Oota, T., Tsurugi, M., Nakagawa, T., Arimoto, H., Hayakawa, M., Tamura, M., Ozaki, Y., and Yamada, Y., Noninvasive near-infrared blood glucose monitoring using a calibration model built by a numerical simulation method: Trial application to patients in an intensive care unit, *Applied Spectroscopy*, Vol. 60, No. 12 (2006), pp. 1423-1431
- (27) Smith, N.T., Wesseling, K.H., and de Wit, B., Evaluation of two prototype devices producing noninvasive, pulsatile, calibrated blood pressure measurement from a finger, *Journal of Clinical Monitoring*, Vol. 1, No. 1 (1985), pp. 17-29.
- (28) Tanaka, G., Sawada, Y., and Yamakoshi, K., Beat-by-beat double-normalized pulse volume derived photoplethysmographically as a new quantitative index of finger vascular tone in humans, *European Journal of Applied Physiology*., Vol. 81, No. 1-2 (2000), pp. 148-154.
- (29) Takeuchi, A., Araki, R., Proskurin, S.G., Takahashi, Y., Yamada, Y., Ishii, J., Katayama, S., and Itabashi, A., A new method of bone tissue measurement based upon light scattering, *Journal of Bone and Mineral Research*, Vol. 12, No. 2 (1997), pp. 261-266.
- (30) Ugryumova, N., Matcher, S.J., and Attenburrow, D.P., Measurement of bone mineral density via light scattering, *Physics in Medicine and Biology*, Vol. 49, No. 3 (2004), pp. 469-483.
- (31) Tanaka, S.M., Nogawa, M., Yamakoshi, K., and Tsujimoto, T., A novel bone densitometer using near-infrared light, *Japanese Journal of Clinical Biomechanics*, Vol. 28 (2007), pp. 35-40 (in Japanese)
- (32) Bell, E., Ivarsson, B., and Merrill, C., Production of a tissue-like structure by contraction of collagen lattices by human fibroblasts of different proliferative potential in vitro, *Proceedings of the National Academy of Sciences of the United States of America*, Vol. 76, No. 3 (1979), pp. 1274-1278.
- (33) Campbell, B.H., Clark, W.W., and Wang, J.H., A multi-station culture force monitor system to study cellular contractility, *Journal of Biomechanics*, Vol. 36, No. 1 (2003), pp. 137-40.
- (34) Yang, Z., Lin, J.S., Chen, J., and Wang, J.H., Determining substrate displacement and cell traction fields - a new approach, *Journal of Theoretical Biology*, Vol. 242, No. 3 (2006), pp. 607-616.
- (35) Nedelec, B., Ghahary, A., Scott, P.G., and Tredget, E.E., Control of wound contraction. Basic and clinical features, *Hand Clinics*, Vol. 16, No. 2 (2000), pp.289-302.
- (36) Tan, W., Oldenburg, A.L., Norman, J.J., Desai, T.A., and Boppart, S.A., Optical coherence tomography of cell dynamics in three-dimensional tissue models, *Optics Express*, Vol. 14, No. 16 (2006), pp. 7159-7171.
- (37) Bagnaninchi, P.O., Yang, Y., Zghoul, N., Maffulli, N., Wang, R.K., and Haj, A.J., Chitosan microchannel scaffolds for tendon tissue engineering characterized using optical coherence tomography, *Tissue Engineering*, Vol. 13, No. 2 (2007), pp. 323-331.

- (38) Nerella, N.G. and Drennen, J.K., Depth-resolved near-infrared spectroscopy, *Applied Spectroscopy*, Vol. 50, No. 2 (1996), pp. 285-291.
- (39) Troy, T.L., and Thennadil, S.N., Optical properties of human skin in the near infrared wavelength range of 1000 to 2200 nm, *Journal of Biomedical Optics*, Vol. 6, No.2 (2001), pp. 167-176.
- (40) Boutroy, S., Buxsein, M.L., Munoz, F., and Delmas, P.D., In vivo assessment of trabecular bone microarchitecture by high-resolution peripheral quantitative computed tomography, *The Journal of Clinical Endocrinology and Metabolism*, Vol. 90, No. 12 (2005), pp. 6508-6515.